

1 EXPERIMENTAL: GANCICLOVIR NANOPARTICLES

1.1 MATERIALS

Ganciclovir was obtained as a gift sample from Ranbaxy (super speciality) Pvt. Ltd., Himachal Pradesh, India. Chitosan (Medium molecular weight) was purchased from Sigma Aldrich (St. Louis, MO). Sodium hyaluronate and sodium tri poly phosphate (TPP) were purchased from Himedia, Mumbai, India. Sodium fluorescein was purchased from Sigma Aldrich, USA. Chloroform (HPLC Grade) and Methanol (HPLC Grade) were purchased from Merck, Mumbai, India. Potassium dihydrogen phosphate, sodium hydroxide, sodium chloride and all other analytical reagents were obtained from S.D. fine-chem limited, Baroda, India. All the reagents used were of analytical grade. Cellulose dialysis tubing (Molecular weight cut of 12000; pore size 0.4nm) and membrane filter of pore size 0.2 μm were purchased from Himedia Lab, Mumbai, India. Distilled water used in the study was filtered using 0.22- μm nylon filter (Nylon N66 membrane filters 47 mm, Rankem, India).

1.2 EQUIPMENTS

Analytical weighing balance (Shimadzu, Switzerland)

High speed magnetic stirrer (Remi, MS500, Remi equipments, Mumbai, India)

High speed Centrifuge (Sigma 3K30, Germany)

Ultrasonic Bath Sonicator (Ultrasonics Selec, Vetra, Italy)

Particle size Analyzer (Zeta sizer Nano series, Malvern Instruments, UK)

UV-VIS Spectrophotometer (Shimadzu, Japan)

High Pressure Liquid Chromatography (Shimadzu Corporation, Japan)

Lyophilizer (Heto Drywinner, Denmark)

Differential Scanning Calorimeter (Mettler Toledo DSC 822e, Japan)

Transmission Electron Microscope (Morgagni, FEI Company, USA)

Nuclear Magnetic Resonance (^1H NMR) (Bruker Instruments, USA)

Gel Permeation Chromatography (Shimadzu LC-10 A HPLC/GPC system, Japan)

Cyclomixer (Spinix, Tarsons, India)

1.3 METHODS

1.3.1 Preparation of Chitosan hydrochloride salt

Chitosan hydrochloride salt (CS HCl) was prepared from commercial grade medium molecular weight chitosan by slight modification in the reported method of Signini et al., 1999 as per the laboratory set up. The salt was then characterized for average degree of acetylation by ^1H NMR spectroscopy and its molecular weight was determined by gel permeation chromatography.

1.3.2 Preparation of ganciclovir loaded chitosan hydrochloride nanoparticles

Various batches of ganciclovir loaded chitosan hydrochloride nanoparticles (GCV loaded CS HCl NPs) were prepared by ionotropic gelation method described by Funete et al., 2008 with slight modification as per laboratory setup.

For ocular distribution studies, dye loaded nanoparticles were prepared by replacing the drug with sodium fluorescein in the aforementioned procedure.

1.3.3 3^2 factorial design

Various batches of GCV loaded CS HCl nanoparticles were prepared based on the 3^2 factorial design. The independent variables taken were HA: CS HCl ratio (A) and drug loading (B). Particle size (Y_1) and entrapment efficiency (Y_2) were taken as dependent variables.

Quantitative aspects of the effects and relationships among various formulation variables of nanoparticles were investigated using 3^2 factorial design. 3^2 factorial design with a total of 9 experimental runs was selected to optimize the various process parameters at three levels (low, medium, and high, coded as -1, 0, and +1). HA: CS HCl ratio (A) and drug loading (B) were taken as independent variables and their effect was studied on size (Y_1) and % entrapment (Y_2) which were taken as dependent variables. The Design-Expert software (version 9.0.0.7, State-Ease Inc., Minneapolis, USA) was used for design of experiment, analysis of second-order model and for drawing of three dimensional response surface and contour plots. The optimized batch was selected on the basis of desirability criteria. % prediction error of the prepared batch was calculated in order to

evaluate the reliability of developed mathematical models (Sharma et al., 2012). Following formula was used to calculate the % prediction error:

$$\% \text{ Prediction error} = \frac{\text{Actual value} - \text{predicted value}}{\text{Actual value}} \times 100$$

The level and code of variables considered in this study are shown in Table 6.1.

Table 1.1 Variables in 3² factorial design for ganciclovir loaded chitosan hydrochloride nanoparticles

Independent Variables	Units	Coded Values			Response (Y1)	Response (Y2)
		-1	0	1		
HA:CS HCl ratio (A)	w/w	1:2	1:1	2:1	Particle Size (nm)	Encapsulation Efficiency (%)
Drug loading (B)	w/w	5	10	20		

1.3.4 Selection of cryoprotectant for lyophilization of nanoparticles

The optimized GCV loaded CS HCl nanoparticles formulation was lyophilized using lyophilizer (Heto Drywinner, Germany) as per the method described in section 4.3.4 of chapter 4.

1.4 CHARACTERIZATION

1.4.1 Characterization of chitosan hydrochloride salt

1.4.1.1 ¹H Nuclear Magnetic Resonance (¹H NMR)

The prepared chitosan hydrochloride salt was characterized for average degree of acetylation by ¹H NMR spectroscopy by dissolving CS HCl in D₂O/ HCl (100:1v/v) at 80 °C, by using a 200 MHz spectrometer (Bruker Instruments, USA).

1.4.1.2 Molecular Weight Determination

Gel permeation chromatography (GPC)/ Molecular weight distribution was carried out in order to determine the molecular weight of prepared chitosan hydrochloride salt. The number average molecular weight (M_n), weight average molecular weight (M_w) and z-average molecular weight (W_z) was determined by following equations:

➤ **Number Average molecular weight (M_n):**

The number average molecular weight is the statistical average molecular weight of all the polymer chains in the sample, and is defined by:

$$M_n = \frac{\sum NiMi}{\sum Ni}$$

➤ **Weight Average molecular weight (M_w):**

The weight average molecular weight (M_w) is defined by:

$$M_w = \frac{\sum NiMi^2}{\sum NiMi}$$

➤ **Higher average molecular weights (M_z):**

In general, a series of average molecular weights can be defined by equation

$$M = \frac{\sum NiM^{n+1}}{\sum NiMi^n}$$

Where,

n=1 gives M=M_w

n=2 gives M=M_z

n=3 gives M=M_{z+1}

➤ **Polydispersity index:**

The polydispersity index is used as a measure of the broadness of a molecular weight distribution of a polymer, and is defined by:

$$\text{Polydispersity index} = \frac{M_w}{M_n}$$

1.4.1.3 Differential Scanning Calorimetry

Differential Scanning Calorimetry studies of medium molecular weight chitosan and prepared chitosan hydrochloride salt was carried out (DSC-60, Shimadzu, Japan). Sample was sealed in standard aluminum pans with lids and purged with air at a flow rate of 40 ml/min. Temperature ramp speed was set at 20°C /min, and the heat flow was recorded in the range of 30–300 °C under inert nitrogen atmosphere.

1.4.2 Characterization of nanoparticles

1.4.2.1 Determination of particle Size (PS) and Zeta Potential (ζ)

Mean PS and ζ of ganciclovir loaded CS HCl nanoparticles were determined using dynamic light scattering method (Zetasizer NanoZS, Malvern, Worcestershire, UK). The ζ of nanoparticles was measured using the laser Doppler method (Zetasizer Nano ZS). Each batch was analyzed in triplicate. For PS and ζ , analysis was carried out for 100 s and 60s resp. at room temperature by keeping angle of detection at 90°.

1.4.2.2 Encapsulation Efficiency (EE)

The encapsulation efficiency of ganciclovir in nanoparticles was determined by centrifugation technique (Motwani et al., 2006). Similarly, the amount of free drug in supernatant was calculated and finally encapsulation efficiency was calculated by the following formula:

Entrapment efficiency was calculated by the following formula:

$$\% EE = \frac{\text{Total drug} - \text{Free Drug}}{\text{Total drug added to nanoparticle formulation}} \times 100$$

In lyophilized GCV nanoparticles, drug content was determined by dissolving 2mg of obtained lyophilized powder in chloroform: methanol (2:8) and the samples were then analyzed by UV spectrophotometer at 254 nm, after suitable dilutions.

1.4.2.3 Differential Scanning Calorimetry (DSC)

Differential Scanning Calorimetry studies of drug, excipients and lyophilized nanoparticles were carried out (DSC-60, Shimadzu, Japan) in order to define the physical state of drug in nanoparticles and possibility of interaction between the drug and excipients within the nanoparticles. Each sample was sealed in standard aluminum pans with lids and purged with air at a flow rate of 40 ml/min. Temperature ramp speed was set at 20°C /min, and the heat flow was recorded in the range of 30–300 °C under inert nitrogen atmosphere.

Thermograms were taken for GCV, CS HCl, HA, TPP and lyophilized GCV nanoparticles.

1.4.2.4 Transmission electron microscopy (TEM)

TEM analysis of the prepared formulation was carried out to understand the morphology of nanoparticles. A drop of nanoparticles containing 0.01% of phosphotungstic acid was placed on a carbon film coated on a copper grid. TEM studies were performed at 100 kV using Morgagni Transmission Electron Microscope 268 (D) (FEI Company, USA). The copper grid was fixed into sample holder and placed in vacuum chamber of the transmission electron microscope and observed under low vacuum, and TEM images were recorded.

1.4.2.5 *In vitro* release study

In vitro release of GCV from nanoparticles was evaluated by the dialysis bag diffusion technique reported by Motwani et al., 2008. The samples were measured for amount of GCV released using UV method described in section 3.6.1.2 of analytical methods. All the experiments were performed in triplicate, and the average values were taken. GCV solution prepared in PBS (pH 7.4) was used as a control.

1.4.2.6 *Ex vivo* study

Ganciclovir loaded CS HCl nanoparticles were evaluated for corneal permeation characteristics using the isolated goat cornea model (Yadav and Ahuja, 2010).

The apparent permeation coefficient (P_{app} , cm/s) of GCV was determined by reported method of Shen and Tu, 2007.

$$P_{app} Q = \frac{\Delta Q}{\Delta t} \times \frac{1}{AC_0} \times \frac{1}{60} \times 10,000,00$$

Where, CD_0 is the initial concentration of drug in the donor compartment, and A is the area of the cornea. For the calculation of the apparent permeation coefficient in the present study, A was determined as $0.922 \pm 0.31 \text{ cm}^2$. $\Delta Q / \Delta t$ is the steady-state rate of drug permeation across the intact cornea, as obtained from the slope of the straight line relating corneal permeability to time.

1.4.2.7 Stability studies

The stability studies were performed for the lyophilized ganciclovir loaded CS/HA nanoparticles. The samples were kept in transparent glass vials and stored at refrigerated conditions (5- 8°C) and at room temperature (25- 30 °C). At different time points the samples were withdrawn and analyzed for particle size and drug content studies.

1.5 RESULTS AND DISCUSSION

1.5.1 Preparation and characterization of chitosan hydrochloride salt

1.5.1.1 Preparation of chitosan hydrochloride salt

Chitosan is a natural-sourced cationic polymer with unique biological properties including favourable biocompatibility and mucoadhesiveness, and has been extensively studied in drug delivery research. However, chitosan is water-insoluble under physiological pH value, which largely constrains its application. When the molecular weight (MW) of chitosan is decreased by physical, chemical or enzymatic depolymerization, a marvellous improvement of its water-solubility is achieved as a result of the decrease in intramolecular hydrogen bonds (Kubota et al., 2000)

1.5.1.2 Characterization of chitosan hydrochloride salt

➤ Nuclear Magnetic Resonance (^1H NMR)

The region of the ^1H NMR spectrum of chitosan for the determination of its degree of acetylation is shown in Fig. 6.1 with the attribution of signals as done in the literature (Hirari et al., 1991; Rinaudo et al., 1992, Signini et al., 1999).

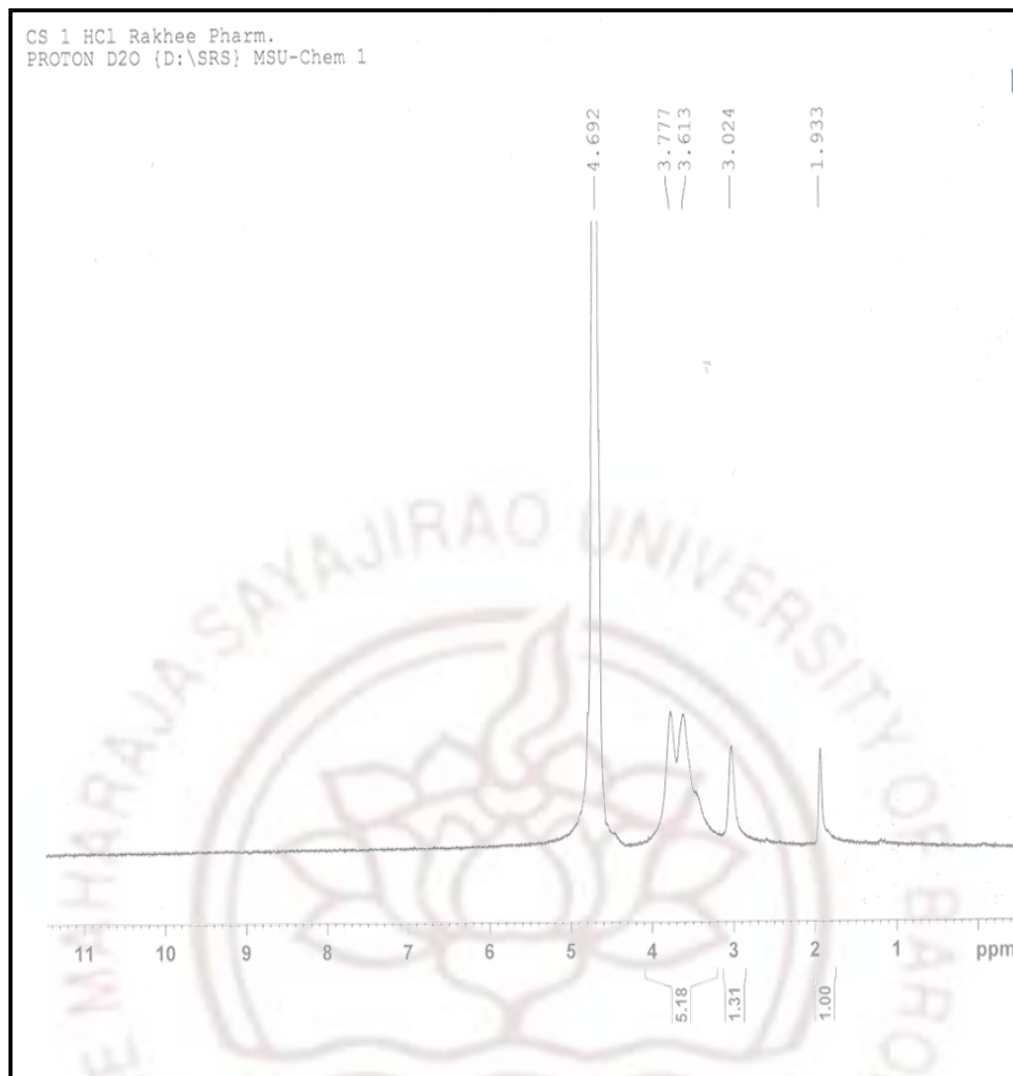


Fig 1.1 ^1H NMR spectra of 1% CS HCl in D_2O /HCl (100:1 v/v) obtained at 80°C

Degree of acetylation was calculated from the expressions given below:

$$\%DA = [(I_{\text{Met}} / 3) / (I_{\text{H}_2})] \times 100 \quad (1)$$

$$\%DA = [(I_{\text{Met}} / 3) / (I_{\text{H}_2}/6 / 6)] \times 100 \quad (2)$$

Degree of acetylation was found to be $29.26 \pm 1.0\%$.

➤ Molecular Weight Determination

The retention time of chitosan hydrochloride in GPC column was found out at 8.439 mins (Fig. 6.2)

The number average molecular weight (M_n), weight average molecular weight (M_w) and molecular weight distribution (M_w/M_n) of chitosan

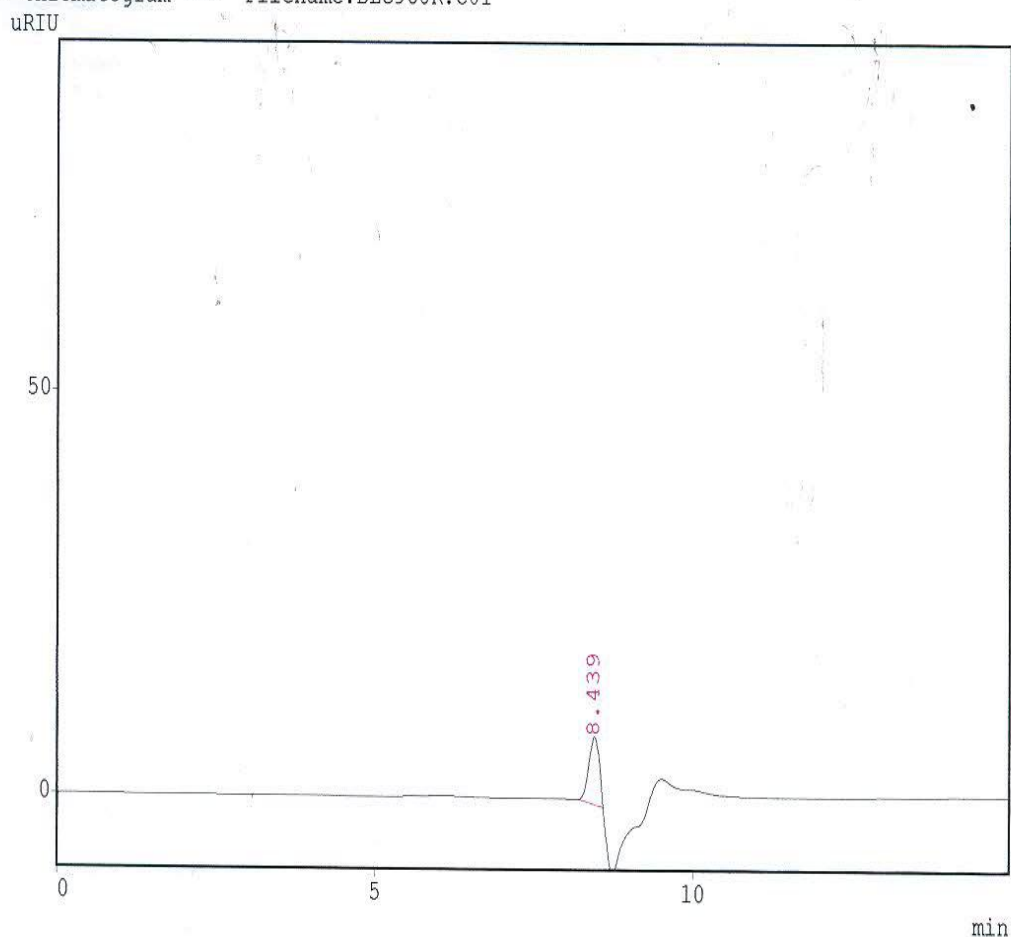
hydrochloride salt was determined by GPC. The average molecular weight (Mn), weight average molecular weight (Mw) and molecular weight distribution (Mw/Mn) was found out to be 3528, 3756 and 1.064, respectively (Table 6.2)

Molecular weight distribution (Mw/Mn) of chitosan hydrochloride salt was found to be 1.06481 which reflects that the synthesized polymer is a monodispersed polymer.



CLASS-LC10 Ver.=1.62 SYS=1 Ch=1 REPORT.NO=2 DATA=BLC968R.D01 13/10/30 14:18:02
 Sample : BLC968 CSHCL 2ML IN WATER
 ID : BUFFER
 Type : Unknown
 Detector : RID-10A
 Operator : CLM/RM
 Method Name : GOKULMET.MET

*** Chromatogram *** Filename:BLC968R.C01



*** Peak Report ***

PKNO	TIME	AREA	HEIGHT	MK	IDNO	CONC	NAME
1	8.439	966144	79105			100.0000	
		966144	79105			100.0000	

Fig 1.2 Gel permeation chromatogram of CS HCl

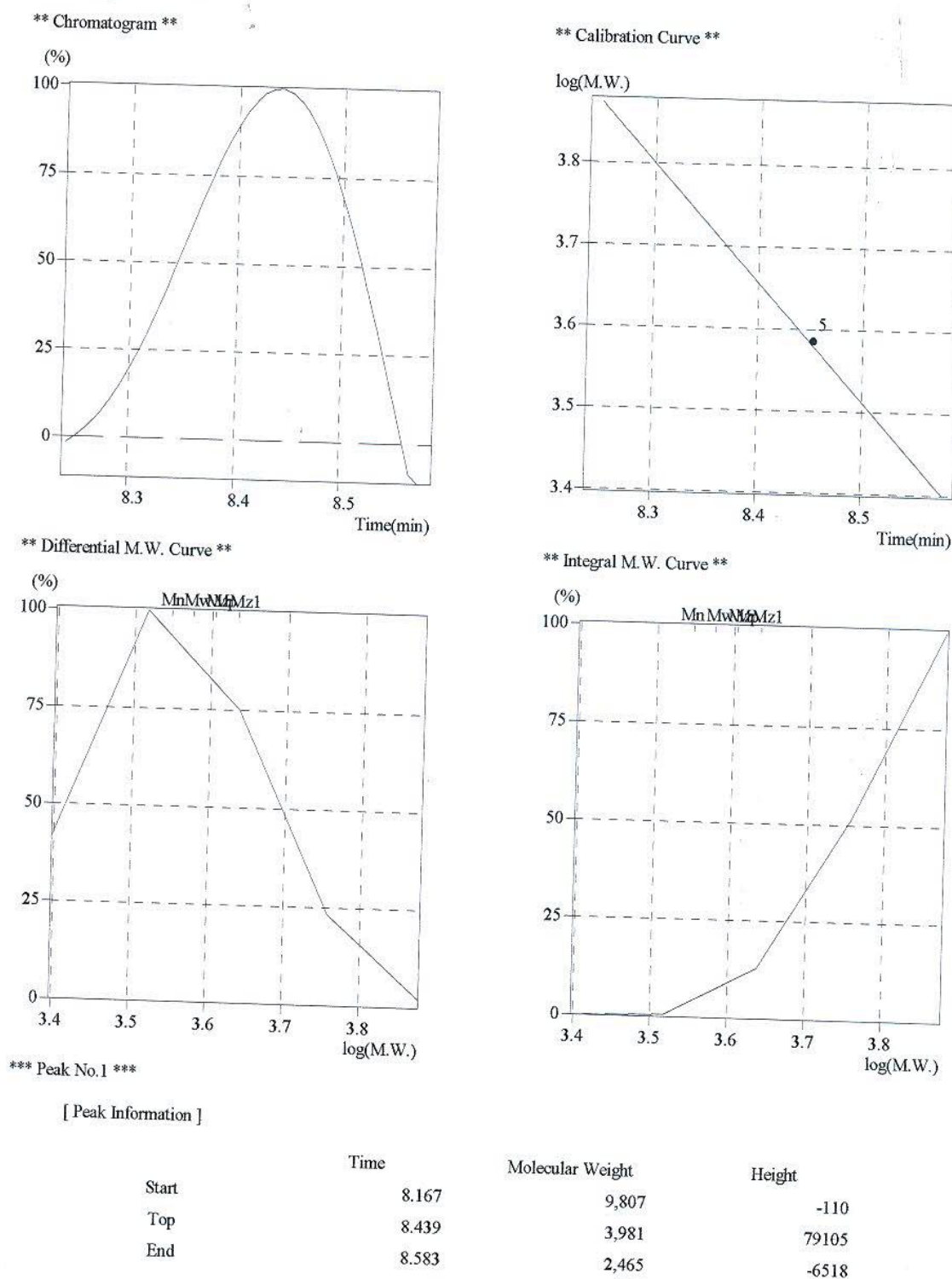


Fig 1.3 Chromatogram, calibration curve, differential M.W. curve and integral M.W. curve of chitosan hydrochloride

Table 1.2 Table showing number, weight and average molecular weight of chitosan hydrochloride salt

[Ave. Molecular Weight]	
Number-A.M.W.(Mn) :	3,528
Weight-A.M.W.(Mw) :	3,756
Z-A.M.W.(Mz) :	4,017
(Z+1)-A.M.W.(Mz1) :	4,305
Mw/Mn	1.06481
Mv/Mn	0.00000
Mz/Mw	1.06927

➤ Differential Scanning Calorimetry

Fig 1.4 DSC thermogram of chitosan

Fig. 6.4 displays thermogram of chitosan (medium molecular weight) and it shows a endothermic peak at 89.97 °C which is attributable to the loss of water and/or due to possible chain relaxation (Martins et al., 2011) and a sharp exothermic peak at around 300 °C which corresponds to CS degradation (Cervera et al., 2004; Liao et al., 2004).

Figure 6.5 shows the thermogram of chitosan hydrochloride salt, it displayed a

Fig.1.5 DSC thermogram of chitosan hydrochloride salt

lower degradation temperature as compared to chitosan and showed a sharp endothermic peak at 223 °C. Aumklad also observed the lower degradation temperature for hydrochloride salts as compared to pure chitosan (Aumklad, 2006).

1.5.2 Preparation and characterization of ganciclovir loaded CS/HA nanoparticles:

1.5.2.1 Preparation of CS/HA nanoparticles:

Nanoparticles with different properties like size, zeta potential, stability and drug loading capacity can easily be formed by ionotropic gelation method (Agnihotri, 2004).

1.5.2.2 Factorial Design

1.5.2.2.1 3² Factorial design

Various batches of ganciclovir loaded CS HCl nanoparticles were prepared according to 3² Design by varying two independent variables HA; CS HCl ratio (A) and drug loading (B). The design matrix of the variables in the coded units along with the results of response variables (size and EE) obtained from each batch is shown in Table 6.3.

Table 1.3 3² factorial design matrix of ganciclovir loaded CS/ HA nanoparticles

Std.	Run	HA: CS	Drug	Size (nm)	Encapsulation
		ratio (w/w) A	loading (w/w) B	Y1	Efficiency (%) Y2
5	1	0	0	132.26±3.21	58.23±2.13
3	2	1	-1	148.14±4.12	52.68±3.43
4	3	-1	0	112.7±3.24	54.9±4.67
8	4	0	1	139.89±5.65	62.68±2.54
2	5	0	-1	124.69±3.12	51.21±3.25
6	6	1	0	155.67±4.32	59.98±3.12
1	7	-1	-1	105.61±3.89	48.43±5.87
10	8	0	0	132.00±4.98	58.36±3.14
9	9	1	1	164.65±4.03	63.57±3.90
7	10	-1	1	121.16±3.12	59.66±4.98
11	11	0	0	132.8±6.54	58.45±2.34

Obtained data of dependent variables (size and encapsulation efficiency) were subjected to multiple regression analysis to yield a second- order polynomial equation (full model), using Design Expert software. This second-order polynomial model helps in relating the responses to selected variables. The data of PS and EE were fitted into equation (1):

$$Y = \beta_0 + \beta_1 A + \beta_2 B + \beta_{12} AB + \beta_{11} AA + \beta_{22} BB \quad \dots\dots\dots (1)$$

where Y represents the measured responses (dependent variable), A and B were the coded values of independent variables, β_0 is the intercept coefficient, β_1 and

β_2 are the linear coefficients, β_{11} and β_{22} are the squared coefficients, and β_{12} is the interaction coefficients.

Table 1.4 ANOVA for the response surface quadratic polynomial model for size

Response	1	Size				
ANOVA for Response Surface Quadratic Model						
Analysis of variance table [Partial sum of squares - Type III]						
	Sum of		Mean	F	p-value	
Source	Squares	Df	Square	Value	Prob > F	
Model	226.35	5	45.27	545.16	< 0.0001	Significant
A-A	29.22	1	29.22	351.83	< 0.0001	
B-B	188.05	1	188.05	2264.5	< 0.0001	
AB	0.029	1	0.029	0.35	0.5809	
A ²	1.97	1	1.97	23.74	0.0046	
B ²	4.80	1	4.80	57.85	0.0006	
Residual	0.42	5	0.083			
Lack of Fit	0.39	3	0.13	10.65	0.0871	not significant
Pure Error	0.0242	2	0.012			
Cor Total	226.77	10				

$R^2=0.9996$; adjusted- $R^2=0.9993$; predicted- $R^2=0.9977$ and Adequate

precision = 168.144

Finally, two equations were obtained for PS and EE:

$$Y_1=132.17+21.45A+7.93B+0.16AB + 2.28A^2+0.38 B^2 \quad \dots\dots\dots (2)$$

$$Y_2=58.34+2.21 A+5.60B-0.085AB-0.88A^2-1.38B^2 \quad \dots\dots\dots (3)$$

Positive and negative sign in front of the terms indicates synergistic and antagonistic effect, respectively. The results of ANOVA of the second-order polynomial equation are given in Tables 6.4 and 6.5 for PS and EE, respectively.

Table 1.5 ANOVA for the response surface quadratic polynomial model for entrapment efficiency

Response	2	Encapsulation efficiency					
ANOVA for Response Surface Quadratic Model							
Analysis of variance table [Partial sum of squares - Type III]							
	Sum of		Mean	F	p-value		
Source	Squares	Df	Square	Value	Prob > F		
Model	3152.56	5	630.51	2817.07	< 0.0001	Significant	
A-A	2759.33	1	2759.33	12328.39	< 0.0001		
B-B	377.31	1	377.31	1685.78	< 0.0001		
AB	0.10	1	0.10	0.46	0.5288		
A ²	13.15	1	13.15	58.74	0.0006		
B ²	0.37	1	0.37	1.66	0.2538		
Residual	1.12	5	0.22				
Lack of Fit	0.79	3	0.26	1.57	0.4114	not significant	
Pure Error	0.33	2	0.17				
Cor Total	3153.68	10					

$R^2=0.9982$; adjusted- $R^2=0.9963$; predicted- $R^2=0.9815$ and Adequate precision=73.346.

1.5.2.2.2 Response surface plots

Three-dimensional response surface plots for PS and EE were generated by the Design Expert software and are presented in Fig. 6.6 and 6.7 for ganciclovir loaded CS/HA nanoparticles respectively.

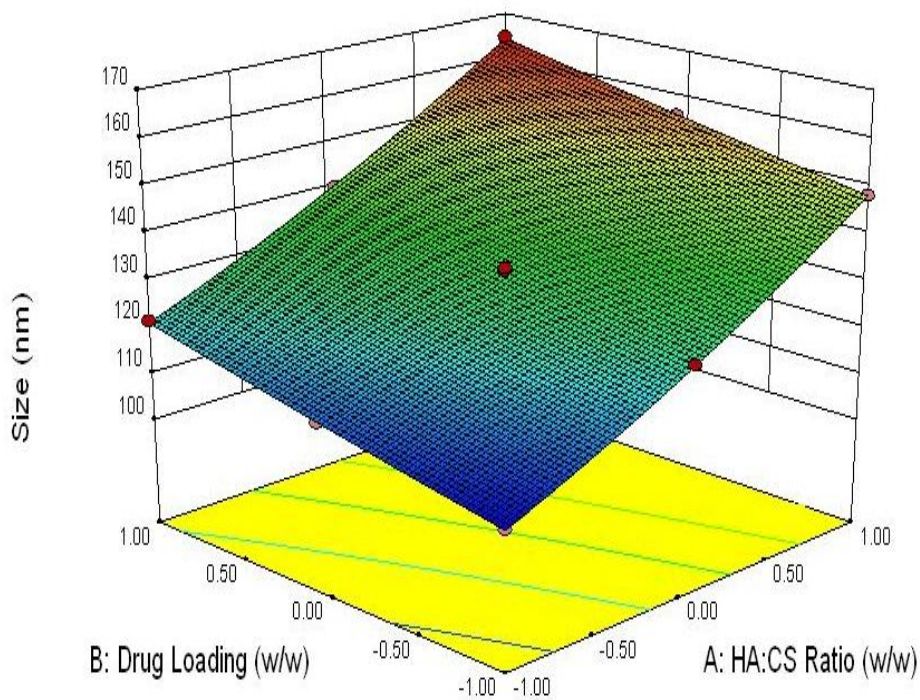


Fig 1.6 Three-dimensional surface plot of HA: CS ratio vs drug loading for size

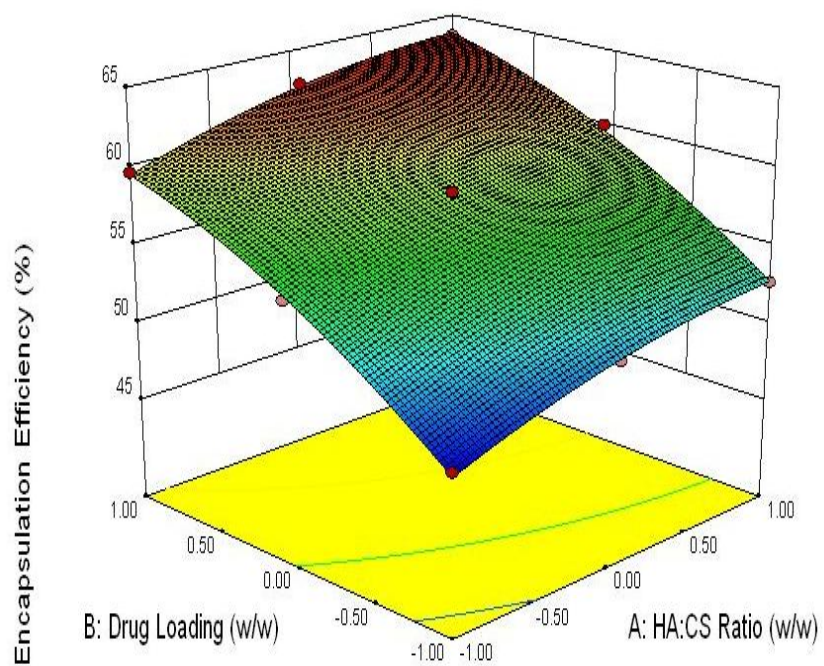


Fig 1.7 Three-dimensional surface plot of HA: CS ratio vs drug loading for entrapment efficiency

1.5.2.2.3 Contour plots

The contour plots are shown in Figs. 6.8 and 6.9. Two parameters of each model were plotted at any one time on the X and Y axes with the yield in Z axis.

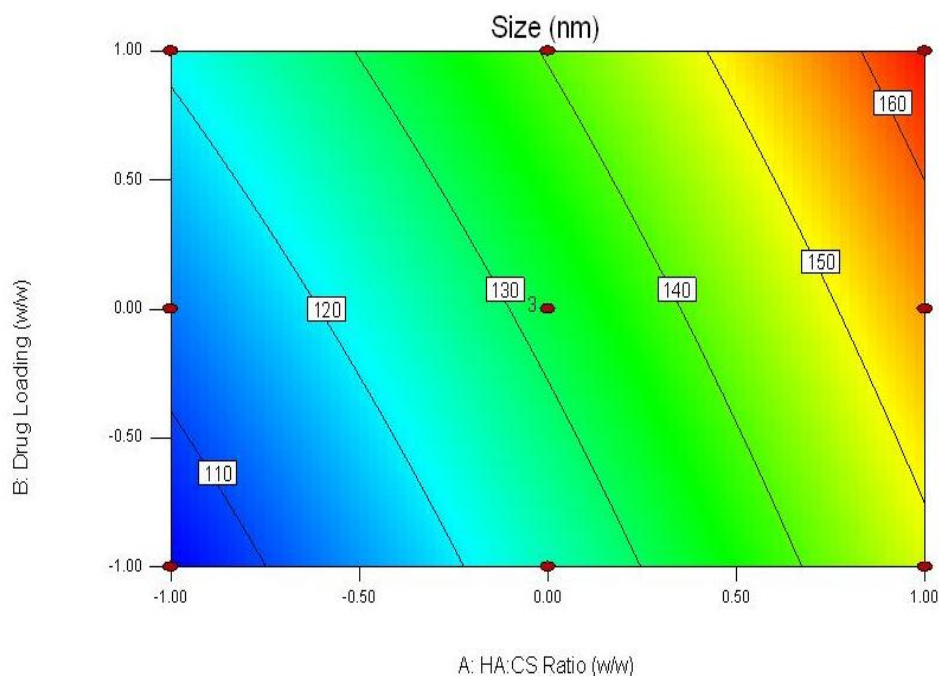


Fig 1.8 Contour plots of HA: CS ratio vs drug loading for size

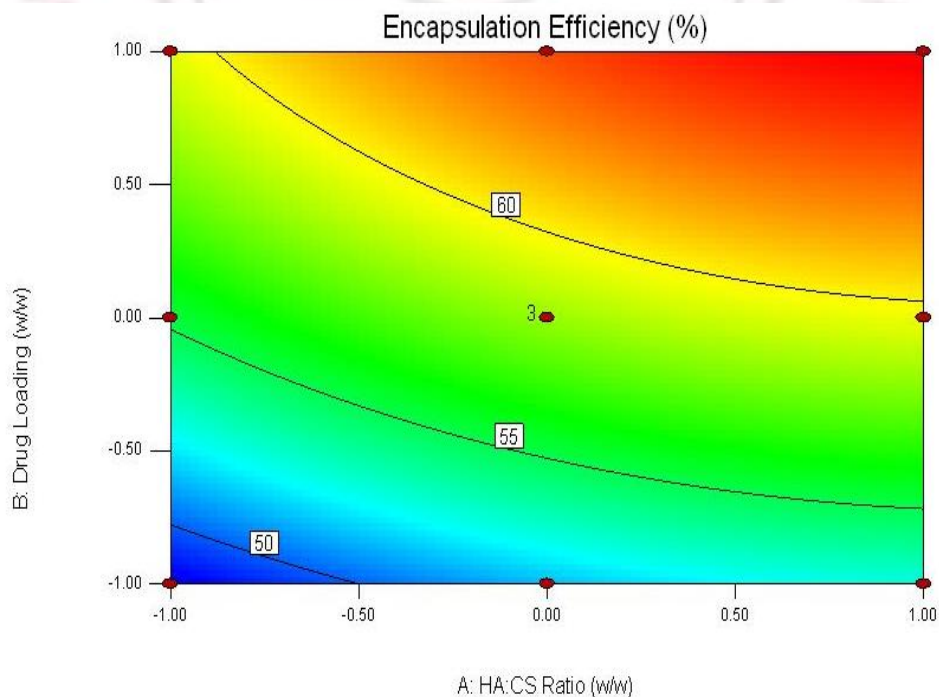


Fig 1.9 Contour plots of nanoparticles of HA: CS ratio vs drug loading for entrapment efficiency

1.5.2.2.4 Selection of optimized batch

The prepared batches of GCV loaded CS/HA nanoparticles, showed a wide variation from 105.61±3.89 to 164.65±4.03nm and 48.43±2.87 to 63.57±3.90 % for PS and EE, respectively (Table 6.3). Moreover, as PS and EE have to be considered simultaneously, the selection of optimized batch was more difficult as the batch with smallest particle size 105.61±3.89 nm exhibited EE of only 48.43±2.87 % (A=-1, B=-1) while the batch with maximum EE 63.57±3.90% have particle size of 164.65±4.03nm (A=1,B=1). Thus, the optimized batch was selected based on overall desirability factor calculated by Design Expert Software.

The results of dependent variables from the software were found to be 121.16± 3.12 nm for particle size and 59.99 ± 3.14 for % EE at these levels which is as per our desired criteria. The calculated desirability factor for offered formulations was 0.736, which was near to 1 and indicates suitability of the designed factorial model.

Using these parameters i.e., A=-1 and B=1, a batch of GCV loaded CS/ HA nanoparticles was prepared, which was found to have the particle size (Y1) of 124.54± 2.91nm, and % EE (Y2) of 61.12 ± 2.76 %.

Predicted error was calculated by using the following formula:

$$\text{Predicted Error (\%)} = \frac{(\text{Observed Value} - \text{Predicted value})}{\text{Predicted Value}} \times 100$$

Table 1.6 Observed and Predicted response variables of GCV loaded CS/HA nanoparticles

The lower values of % prediction error 2.40 % for (Y1) and 1.88 % for (Y2) indicate the reliability of developed mathematical models.

1.5.2.3 Selection of cryoprotectant for lyophilization of emulsomes

The optimized batch of GCV loaded CS HCl nanoparticles was lyophilized using different ratios of sucrose; mannitol and trehalose dehydrate in order to find out optimum ratio of drug: cryoprotectant which showed minimum increase in particle size. The redispersibility of the freeze-dried formulations and particle

size of the nanoparticles before and after freeze-drying was measured and recorded in Table 6.7.

Table 1.7 Effect of different cryoprotectant ratios on particle size and redispersibility of ganciclovir loaded CS HCl nanoparticles

CryoprotectantName and Ratio	Particle size before lyophilisation (Si)	Particle size after lyophilisation (Sf)	Redispersibility (Sf/Si)
Sucrose (1:3)	121.16±3.12 nm	134.65±3.59 nm	1.11
Sucrose (1:5)		143.40±3.81 nm	1.18
Mannitol (1:3)		160.97±2.45 nm	1.32
Mannitol (1:5)		172.35±4.43 nm	1.42
Trehalose dehydrate (1:3)		140.19±3.63 nm	1.15
Trehalose dehydrate (1:5)		149.55±4.14 nms	1.23

Fig 1.10 Average particle size of lyophilized GCV loaded CS/HA nanoparticles

1.5.2.4 Characterization of CS/HA nanoparticles

1.5.2.4.1 Determination of particle size, ζ and entrapment efficiency

Initial studies aiming at the optimization of the nanoparticles formation indicated that reproducible nanoparticles were formed with HA/CS ratios of 1:2 to 2:1. Fig. 6.11 and 6.12 show the particle size distribution and zeta potential of optimized batch of ganciclovir loaded CS HCl nanoparticles respectively.

Fig 1.11 Particle Size distribution of ganciclovir loaded CS/HA nanoparticles

Charge on the surface of nanoparticles varied with HA concentration in HA/CS nanoparticles. Surface charges were positive when nanoparticles were prepared in 1:2 and 1:1 ratios of HA/CS ratio while the zeta potential value

inverted to negative when HA/CS ratio was 2:1. The zeta potential value of optimized batch was 35.45 ± 2.13 mV (Fig. 6.12).

Fig 1.12 Zeta potential of ganciclovir loaded CS /HA nanoparticles

For ocular distribution studies, dye loaded CS HCl nanoparticles were prepared by incorporating sodium fluorescein in nanoparticles instead of GCV. The mean particle size of sodium fluorescein loaded nanoparticles was 123.71 ± 3.14 nm.

1.5.2.4.2 Determination of Encapsulation Efficiency

Entrapment efficiencies of the prepared batches were in the range of 48.43 ± 2.87 to 63.57 ± 3.90 %. The optimized batch of CS/HA NPs had entrapment efficiency of 61.12 ± 2.76 %.

1.5.2.4.3 Differential Scanning Calorimetry

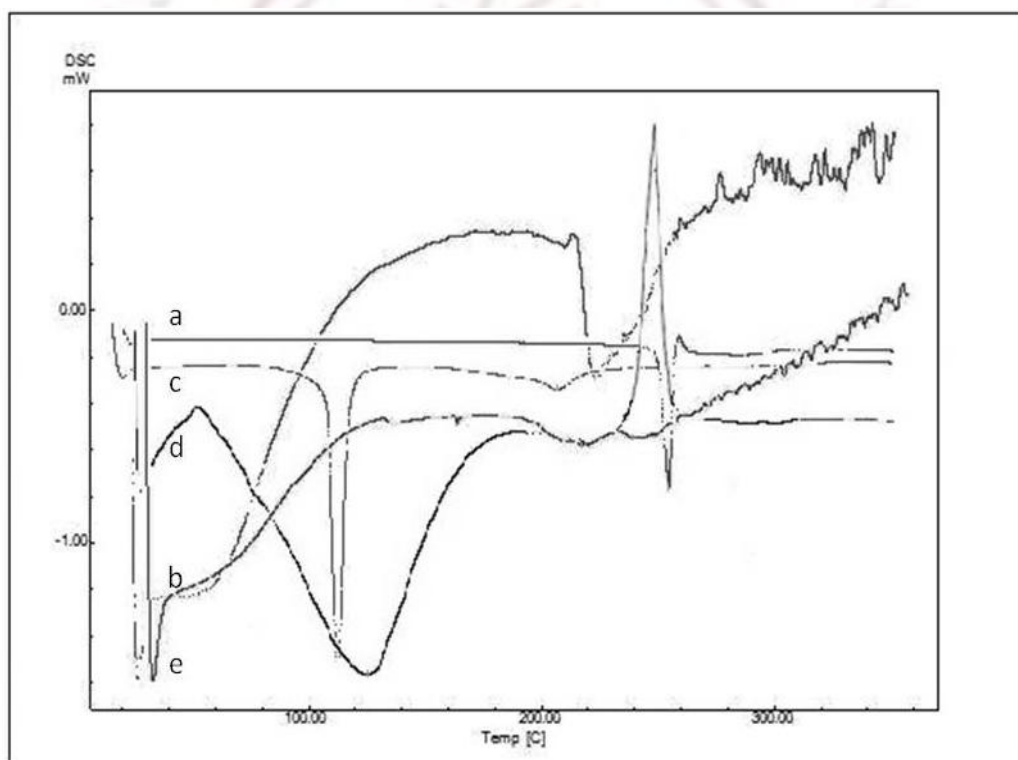


Fig 1.13 DSC thermogram of a) ganciclovir, b) chitosan hydrochloride, c) TPP, d) HA, e) CS/HCl nanoparticles

DSC studies were performed on GCV, excipients (chitosan, chitosan HCl salt, TPP, HA) and GCV loaded nanoparticles. Transmission Electron Microscopy

The shape of the CS HCl/ HA nanoparticles was investigated using transmission electron microscopy (TEM). CS HCl/HA nanoparticles were seen to be distinct, spherical particles with solid dense structure (Fig. 6.14).

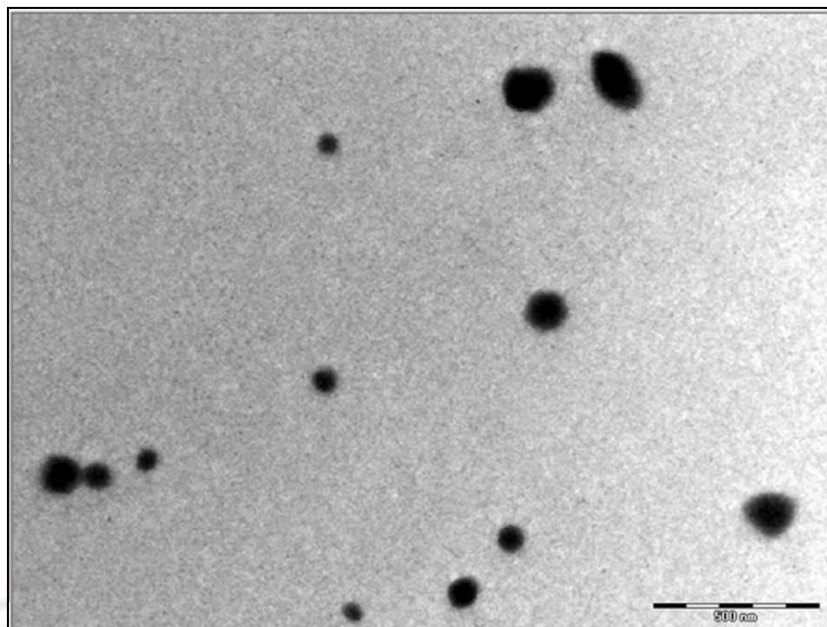


Fig 1.14 TEM image of ganciclovir loaded CS HCl nanoparticles

1.5.2.4.4 *In vitro* drug release studies

The *in vitro* release of ganciclovir from its aqueous solution and CS/HA nanoparticles was investigated in phosphate buffer saline at $37 \text{ }^{\circ}\text{C} \pm 2 \text{ }^{\circ}\text{C}$. Fig. 6.15 displays the release profile of GCV aqueous solution and GCV CS/HA nps.

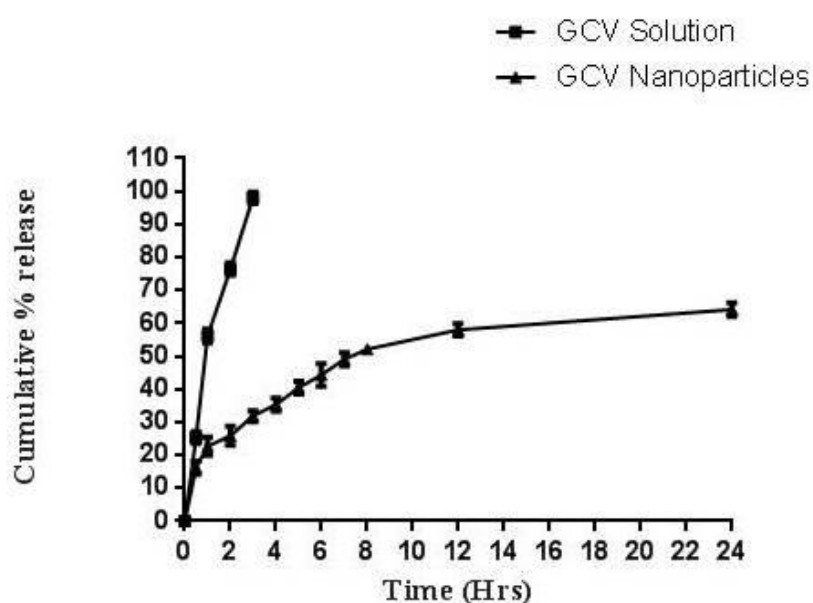


Fig 1.1 5 Release profile of ganciclovir from solution and CS /HA nanoparticles

1.5.2.4.5 Ex vivo studies

Table 6.8 compares the results of *ex vivo* corneal permeation of ganciclovir from the nanoparticles with ganciclovir solution across isolated goat cornea.

Table 1.8 Ex vivo permeation of ganciclovir from nanoparticles and aqueous solution

S. No.	Formulations	Corneal Permeation (cm/s)
1	Ganciclovir loaded CS HCl nanoparticles	4.53±0.43
2	Ganciclovir solution	1.29± 0.89

1.5.2.4.6 Stability Studies

The data of stability studies of lyophilized GCV loaded CS HCl nanoparticles at refrigerated conditions (2-8°C) and at room temperature (25-30 °C) are shown in Table 6.9

Table 1.9 Stability profile of lyophilized GCV loaded nanoparticles at 2-8° C and 25- 30 °C

1.6 REFERENCES

- Agilent Technology. Polymer molecular weight distribution and definitions of MW averages, Technical Overview.
- Agnihotri SA, Mallikarjuna NN, Aminabhavi TM. Recent advances on chitosan-based micro- and nanoparticles in drug delivery. *J. Control Release.* 100, 2004, 5-28.
- Arai K., Kinumaki T, Fujita T. Toxicity of chitosan. *Bull. Tokai Reg. Fish Lab.* 43, 1968, 89-94.
- Aumklad P. Effect of molecular weight and salt forms of chitosan on Epithelial permeability using caco-2 cells (thesis). 2006, ISBN 974 - 11 - 6239 - 1.
- Bishop P. The biochemical structure of mammalian vitreous. *Eye.* 10, 1996, 664-670.
- Cervera MF, Heinamaki J, Krogars K, Jorgenson AC. Solid state and mechanical properties of aqueous chitosan-Amylose starch films plasticized with polyols, *AAPS pharm sci Tech.* 5, 2004, 1-6.
- Chacon M, Molpeceres J, Berges L, Guzman M, Aberturas MR. Stability and freeze-drying of cyclosporine loaded poly (dl-lactideglycolide) carriers. *Eur. J. Pharm. Sci.* 8, 1999, 99-107.
- Csaba N, Höggård MK, Alonso MJ. Ionically crosslinked chitosan/tripolyphosphate nanoparticles for oligonucleotide and plasmid DNA delivery. *Int J Pharm.* 382, 2009, 205-214.
- De la Fuente M, Seijo B, Alonso MJ. Bioadhesive hyaluronan-chitosan nanoparticles can transport genes across the ocular mucosa and transfect ocular tissue, *Gene Ther.* 15, 2008, 668-676.
- Di Colo G, Zambito Y, Burgalassi S, Nardini I, Saettone MF. Effect of chitosan and of *N*-carboxymethylchitosan on intraocular penetration of topically applied ofloxacin. *Int. J. Pharm.* 273, 2004, 37-44.
- Fernandez MJA, Freire DLF, Rey MBS. Hyaluronic acid nanoparticles. *US* 2006/0188578 A1
- Hiari A, Odani H, Nakajima A. Determination of degree of deacetylation of chitosan by ^1H NMR spectroscopy. *Polym. Bull.* 26, 1991, 87-94.

- Jaeghere FD, Allemann E, Leroux JC, Stevels W, Feijen J, Doelker E, Gurny R. Formulation and lyoprotection of poly (lactic acid-co-ethylene oxide) nanoparticles: influence on physical stability and in vitro cell uptake. *Pharm. Res.* 16, 1999, 859–866.
- Janes K. and Alonso MJ. Depolymerized chitosan nanoparticles for protein delivery: preparation and characterization. *J. Appl. Polym. Sci.* 12, 2003, 2769–2776.
- Kubota N, Tatsumoto N, Sano T, Toya K. A simple preparation of half N-acetylated chitosan highly soluble in water and aqueous organic solvents. *Carbohydr. Res.* 324, 2000, 268-274.
- Laurent TC and Fraser JR. Hyaluronan. 6, 1992, 2397–2404.
- Li J, Du Y, Yang J, Feng T, Li A, Chen P. Preparation and characterisation of low molecular weight chitosan and chito-oligomers by a commercial enzyme. *Polym Degrad Stabil.* 87, 2005, 441-448.
- Li N, Zhuanga C, Wang M, Sunb X, Niea S, Pan W. Liposome coated with low molecular weight chitosan and its potential use in ocular drug delivery. *Int J Pharm.* 379, 2009, 131–138.
- Liao SK, and Hung CC. A kinetic study of thermal degradation of chitosan/polycaprolactam blends. *Macromolecular research.* 12, 2004, 466-473.
- Martins AF, Pereira AGB, Fajardo AR, Rubira AF. Characterization of polyelectrolytes complexes based on N,N,N-trimethyl chitosan/heparin prepared at different pH conditions. *Carbohydr. Polym.* 86, 2011, 1266–1272.
- Motwani SK, Khar RK, Ahmad FJ, Chopra S, Kohli K, Talegaonkar S, Iqbal Z. Stability indicating high-performance thinlayer chromatographic determination of gatifloxacin as bulk drug and from polymeric nanoparticles. *Anal. Chim. Acta.* 576, 2006, 253–260.
- Motwani SK, Chopra S, Talegaonkar S, Kohli K, Ahmad FJ, Khar RK. Chitosan–sodium alginate nanoparticles as submicroscopic reservoirs for ocular delivery: Formulation, optimization and in vitro characterization. *Eur J Pharm Biopharm.* 68, 2008, 513-525.

- Paolicelli P, Prego C, Sanchez A, Alonso MJ. Surface-modified PLGA based nanoparticles that can efficiently associate and deliver virus-like particles. *Nanomedicine (Lond)*. 5, 2010, 843-53.
- Polexe RC and Delair T. Elaboration of Stable and Antibody Functionalized Positively Charged Colloids by oyelectrolyte Complexation between Chitosan and Hyaluronic Acid. *Molecules*. 18, 2013, 8563-8578.
- Prabha S, Zhou WZ, Panyam J, Labhasetwar V. Size-dependency of nanoparticle-mediated gene transfer: studies with fractionated nanoparticles. *Int. J. Pharm.* 244, 2002, 105-115.
- Rinaudo M, Le Dung P, Gey C, Milas M. Substituent distribution on O,N-carboxymethylchitosans by ¹H and ¹³C n.m.r. *Int J Biol Macromol*. 14, 1992, 122-128.
- Seyfarth F, Schliemann S, Elsner P, Hipler UC. Antifungal effect of high and low-molecular-weight chitosan hydrochloride, carboxymethyl chitosan, chitosan oligosaccharide and *N*-acetyl-d-glucosamine against *Candida albicans*, *Candida krusei* and *Candida glabrata*. *Int. J. Pharm.* 353, 2008, 139–148.
- Sharma R, Ahuja M, Kaur H. Thiolated pectin nanoparticles: Preparation, characterization and ex vivo corneal permeation study. *Carbohydr Polym*. 87, 2012, 1606– 1610.
- Shen Y, Tu J. Preparation and Ocular Pharmacokinetics of Ganciclovir Liposomes. *AAPS J*. 9, 2007, E371-377.
- Signini R, Filho SPC. On the preparation and characterization of chitosan hydrochloride. *Polymer Bulletin*. 42, 1999, 159-166.
- Yadav M and Ahuja M. Preparation and evaluation of nanoparticles of gum cordia, an anionic polysaccharide for ophthalmic delivery. *Carbohydr Polym*. 81, 2010, 871-877.
- Zimmermann E, Muller RH, Mader K. Influence of different parameters on reconstitution of lyophilized SLN. *Int. J. Pharm.* 196, 2000, 211–213.

